

# How to Design a Good Vibration Sensor Enclosure Using Modal Analysis

Richard Anslow, System Applications Engineer

## Abstract

A well-constructed mechanical enclosure design for a MEMS accelerometer will ensure that high quality vibration data for CbM is extracted from the monitored asset. The mechanical enclosure used to house a MEMS accelerometer needs to have a frequency response better than the integrated MEMS. This article uses modal analysis to provide the natural frequencies possible with enclosure designs. Guidance on vibration sensor design is provided using theoretical and ANSYS modal simulation examples. It is shown that geometry effects, such as enclosure shape (such as a cylinder or a rectangle), and height dominate the natural frequencies in enclosure design. Mechanical design examples are provided for housing single-axis and triaxial MEMS accelerometers with 21 kHz resonant frequency. This article also provides guidance on epoxy integration in enclosures, as well as cable installation and mounting options for sensors.

## What Is Modal Analysis and Why Is It Important?

A steel or aluminum enclosure is used to house a MEMS vibration sensor and provide solid attachment to monitored assets as well as water and dust resistance (IP67). A good metallic enclosure design will ensure high quality vibration data is measured from the asset. Designing a good mechanical enclosure requires an understanding of modal analysis.

Modal analysis is used to understand the vibration characteristics of structures. Modal analysis provides the natural frequencies and normal modes (relative deformation) of a design. The primary concern in modal analysis is to avoid resonance, where the natural frequencies of a structural design closely match that of the applied vibration load. For vibration sensors, the natural frequencies of the enclosure must be greater than that of the applied vibration load measured by the MEMS sensor.

The frequency response plot for the [ADXL1002](#) MEMS accelerometer is shown in Figure 1. The ADXL1002 3 dB bandwidth is 11 kHz, and it has a 21 kHz resonant frequency. A protective enclosure used to house the ADXL1002 needs to have a first natural frequency of 21 kHz or greater.

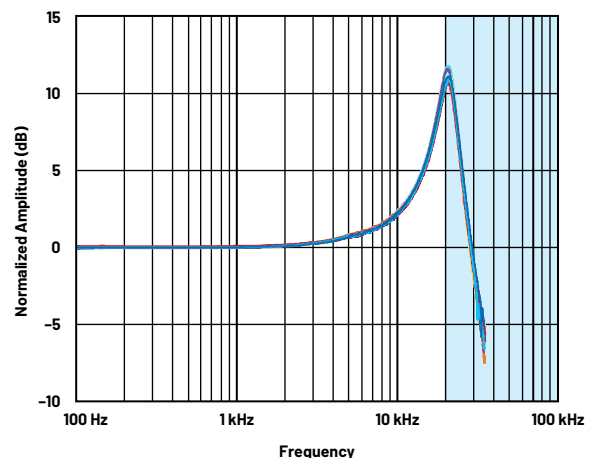


Figure 1. The ADXL1002 MEMS accelerometer frequency response.

## Vibration Sensor Enclosure Model

For modal analysis and design, a vibration sensor can be seen as a thick, short, cantilevered beam cylinder. In addition, the Timoshenko equation of vibration will be used for the simulation. We will cover this in more detail later in the article. A thick, short, cantilevered cylinder is similar to a vibration sensor mounted on industrial equipment, as shown in Figure 2. The vibration sensor is fixed to industrial equipment using a stud mount. Both stud mounting and enclosure design require careful characterization so that mechanical resonances

do not affect the MEMS vibration frequencies of interest. Finite element methods (FEMs) using ANSYS or similar programs can be used as an efficient solver for the equation of vibration of a short, thick cylinder.

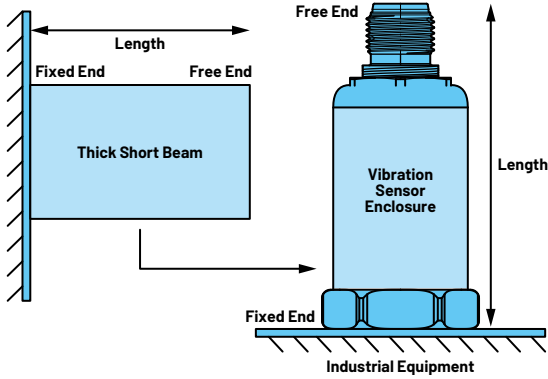


Figure 2. Vibration sensor enclosure modeling.

## Simulation Tools

For modal analysis, ANSYS and other simulation tools assume harmonic motion for every point in the design. The displacement and acceleration of all points in a design are solved as eigenvalues and eigenvectors—in this case, natural frequencies and mode shapes.

### Natural Frequency and Mode Shape

The mass matrix  $M$ , stiffness matrix  $K$ , angular frequency  $\omega_i$ , and mode shape  $\{\Phi_i\}$  are related by Equation 1, which is used in FEM programs like ANSYS.<sup>1</sup> The natural frequency  $f_i$  is calculated by dividing  $\omega_i$  by  $2\pi$ , and the mode shape  $\{\Phi_i\}$  provides the relative deformation patterns of the material at specific natural frequencies.

$$([K] - \omega_i^2 [M]) \{\phi_i\} = \{0\} \quad (1)$$

For a single degree of freedom system, the frequency is simply expressed by:

$$\omega = \sqrt{\frac{K}{M}} \quad (2)$$

Equation 2 provides a simple, intuitive way to evaluate a design. As you reduce the height of the sensor enclosure, the stiffness increases and the mass decreases—therefore, the natural frequency increases. Also, as you increase the height of the enclosure, the stiffness reduces and the mass increases, resulting in a lower natural frequency.

Most designs have multiple degrees of freedom. Some designs have hundreds. Using the FEM provides quick calculations for Equation 1, which would be very time consuming to do by hand.

## Mode Participation Factor

The mode participation factor (MPF) is used to determine which modes and natural frequencies are the most important for your design. The mode shape  $\{\Phi_i\}$ , mass matrix  $M$ , and excitation direction vector  $D$  are related by Equation 3<sup>1</sup> solving for MPF. The square of the participation factor is the effective mass.

$$\gamma_i = \{\phi_i\}_i [M] \{D\} \quad (3)$$

The MPF and effective mass measure the amount of mass moving in each direction for each mode. A high value in a direction means the mode will be excited by forces, such as vibration, in that direction.

Using the MPF in conjunction with the natural frequency will enable the designer to identify potential design problems. For example, the lowest natural frequency produced by a modal analysis may not be the biggest design problem, as it may not have as large a participation factor in your direction of interest (x-, y-, or z-axis plane) relative to all other modes.

The examples shown in Table 1 illustrate that while a 500 Hz natural frequency is predicted in simulation for the x-axis, the mode is weakly excited and is unlikely to be a problem. An 800 Hz strong mode is excited in the enclosure x-axis and will be a problem if the MEMS sensitive axis is orientated in the enclosure x-axis. However, this x-axis strong mode at 800 Hz is not of interest if the designer has their MEMS sensor PCB orientated to measure in the enclosure z-axis.

**Table 1. Natural Frequency (Freq.), Mode Participation Factor (MPF), and Axis of Interest**

Mode	Freq. (Hz)	Axis	MPF	MPF Comment
1	500	X	0.001	Weak mode
2	800	X	0.45	Strong mode
3	1500	Y	0.6	Strong mode
4	3000	Y	0.002	Weak mode
5	10,000	Z	0.33	Strong mode

### Interpreting the Modal Analysis Results

From the previous section we know that modal analysis will tell you what the natural frequencies are in your axis of interest. In addition, the MPF will enable the designer to decide if a frequency can be ignored in a design. To complete the interpretation of modal analysis, it's important to understand that all points on a structure vibrate at the same frequency (global variable), but the amplitude of vibration (or mode shape) at each point is different. For example, an 18 kHz frequency can affect the top of the mechanical enclosure more than the bottom. The mode shape (local variable) has a stronger amplitude at the top of the enclosure compared to the bottom, as shown in Figure 3. This means that while

the enclosure structure top part is strongly excited by an 18 kHz frequency, the MEMS sensor at the enclosure bottom will also be affected by this frequency, though to a lesser degree.

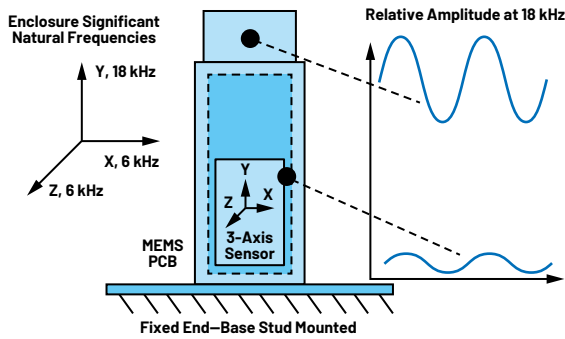


Figure 3. A vibration sensor enclosure's natural frequency, mode shape in axis of interest, and relative amplitude at the top and bottom of the enclosure.

## Timoshenko Differential Equation of Vibration

The Timoshenko equation is suitable for modeling thick, short beams or beams subject to multikilohertz vibration. A vibration sensor, as shown in Figure 2, is analogous to a thick, short cylindrical cross section, which can be modeled using the Timoshenko equation. The equation is a fourth-order differential equation with analytical solutions for restricted cases. The FEM, as presented in Equation 1 to Equation 3, provides the most convenient method of solving the Timoshenko equation using multidimensional matrices, which scale with the number of degrees of freedom of the design.

### Governing Equation

While FEM provides significant benefits in solving the Timoshenko equation of vibration in an efficient manner, an understanding of the trade-offs in designing a vibration sensor enclosure requires closer examination of the Equation 4<sup>2</sup> parameters.

$$EI \frac{\partial^4 y}{\partial x^4} - \rho A \omega^2 y + \left( pI + \frac{\rho EI}{kG} \right) \omega^2 \frac{\partial^2 y}{\partial x^2} + \frac{\rho^2 I}{kG} \omega^4 y = 0 \quad (4)$$

Using different materials or geometries will affect the natural frequency ( $\omega$ ) of the designed structure.

### Material and Geometry Dependencies

The Timoshenko equation parameters can be grouped as either geometry dependent or material dependent.

#### Material dependencies are:

- ▶ Young's modulus (E): this is a measure of the elasticity of a material—how much tensile force is required to deform it. A tensile deforming force occurs at right angles to a surface.
- ▶ Shear modulus (G): this is a measure of the shear stiffness of a material—the ability of an object to withstand a shear stress deforming force when applied parallel to a surface.
- ▶ Material density ( $\rho$ ): mass per unit volume.

#### Geometry dependencies are:

- ▶ Shear coefficient (k): while shear is a material property, the shear coefficient accounts for the variation of shear stress across a cross section. This is typically equal to 5/6 for a rectangular and 9/10 for a circular cross section.
- ▶ Area moment of inertia (I): a geometrical property of an area that reflects how the geometry is distributed around an axis. This property provides insight into a structure's resistance to bending due to an applied moment. In modal analysis this could be considered as resistance to deformation.
- ▶ Cross-sectional area (A): the cross-sectional area of a defined shape, such as a cylinder.

The Timoshenko equation predicts a critical frequency,  $f_c$ , given by Equation 5.<sup>3</sup> As Equation 4 is fourth order, there are four independent solutions below  $f_c$ . For analytical purposes, the Equation 5  $f_c$  is useful for comparing different enclosure geometries and materials.

$$f_c = \frac{1}{2\pi} \sqrt{\frac{kGA}{\rho I}} \quad (5)$$

There are a variety of approaches and solutions to determine all frequencies below  $f_c$ . Some approaches are noted in "Free and Forced Vibrations of Timoshenko Beams Described by Single Difference Equation"<sup>3</sup> and "Flexural Vibration of Propeller Shafts Using Distributed Lumped Modeling Technique."<sup>4</sup> These approaches involve multidimensional matrices, like the FEM.

## What Material Should I Use for My Design?

Table 2 details some common industrial metallic materials such as stainless steel and aluminum.

Copper is the heaviest material of all four listed, and it doesn't provide any advantage over stainless steel, which is lighter, stronger, and less expensive.

Aluminum is a good choice for weight sensitive applications. Its density is 66% less than steel. The downside is that aluminum costs 20× steel per kilogram. Steel is the clear choice for cost sensitive applications.

Although titanium is about two-thirds heavier than aluminum, its inherent strength means that you need less of it. However, using titanium is cost prohibitive for all but the most specialized weight saving applications.

**Table 2. Young's Modulus (E), Shear Modulus (G), Density ( $\rho$ ), and Cost per kg of Common Industrial Metals**

Material	E (N/m <sup>2</sup> )	G (N/m <sup>2</sup> )	$\rho$ (kg/m <sup>3</sup> )	\$ per kg
Stainless steel	2E11	7.7E10	7850	0.11
Copper	1.1E11	4.5E10	8300	9.06
Aluminum	7.1E10	2.4E10	2770	2.18
Titanium	9.6E10	3.6E10	4620	25

### Simulation Example

Figure 4 shows a rectangular metallic vibration sensor enclosure design, with 40 mm height, and 43 mm length by 37 mm width. For modal analysis, the bottom surface (z, x) is a fixed constraint.

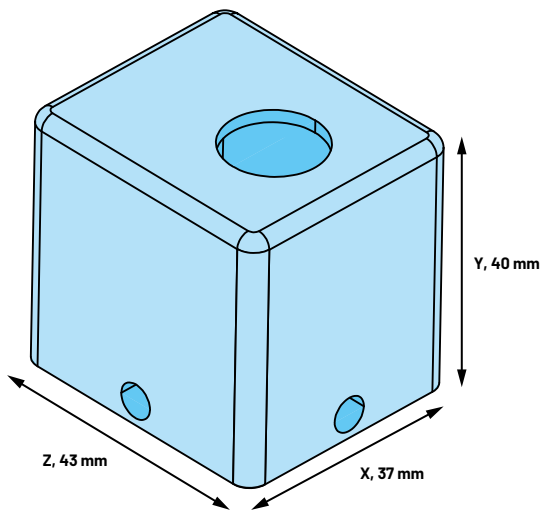


Figure 4. Rectangular enclosure with material type changed for simulation study.

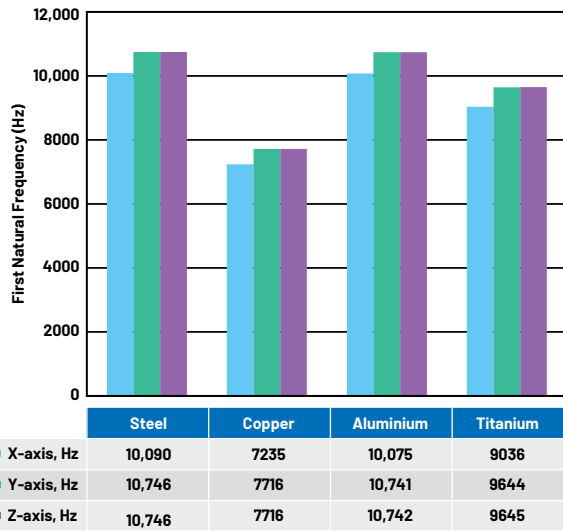


Figure 5. Rectangular enclosure with material type and first significant natural frequency (Hz).

Figure 5 shows modal FEM analysis results for various enclosure materials. The first natural frequency with significant MPF (greater than 0.1 for the ratio of effective mass to total mass of the system) is plotted vs. material type. It's clear that aluminum and stainless steel have the highest first significant natural frequency. They are also good material choices for low cost or low weight applications.

## Should I Design a Rectangular or a Cylindrical Enclosure?

Figure 6 shows both a hollow rectangular and cylindrical stainless steel extrusion, with 2 mm wall thickness and 40 mm height. The outer diameter of the cylinder is 43 mm, and the rectangular piece is also 43 mm on both x and y axes.

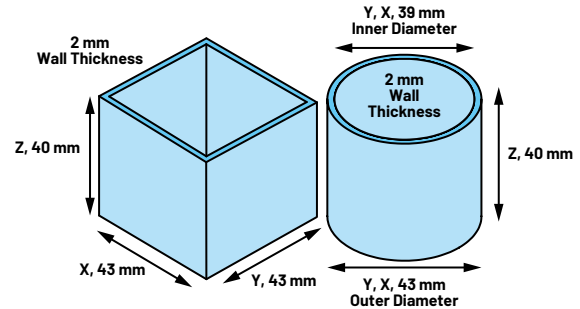


Figure 6. Similar rectangular and cylindrical shapes for modal design study.

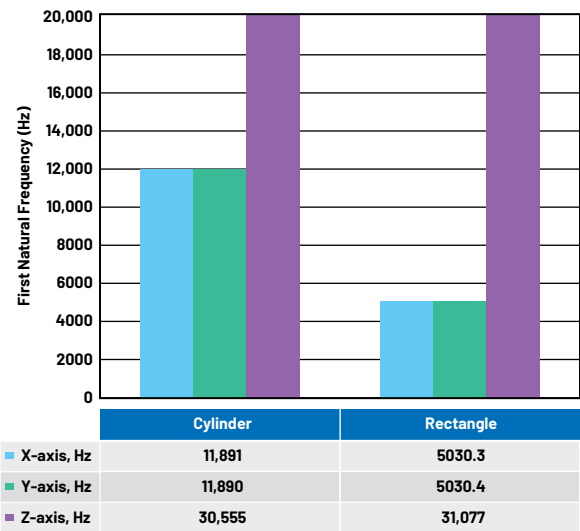


Figure 7. First significant natural frequency (Hz) for similar rectangular and cylindrical shapes.

For modal analysis, the entire 2 mm wall surface (or x, y cross-sectional area) is a fixed constraint. Figure 7 shows modal FEM analysis results. The first natural frequency with significant MPF (greater than 0.1 for the ratio of effective mass to total mass of the system) is plotted vs. material shape. The cylindrical shape has the highest first significant natural frequency for x and y axes, with similar performance in the z direction.

## Geometry—Area and Inertia

Equation 4 includes both material and geometric dependencies. As both rectangular and cylindrical pieces were simulated using stainless steel parameters, the only reason for better performance with the cylindrical piece is geometry. Figure 8 illustrates the cylinder and rectangle cross section for calculation of the area moment of inertia and cross-sectional area of the pieces.

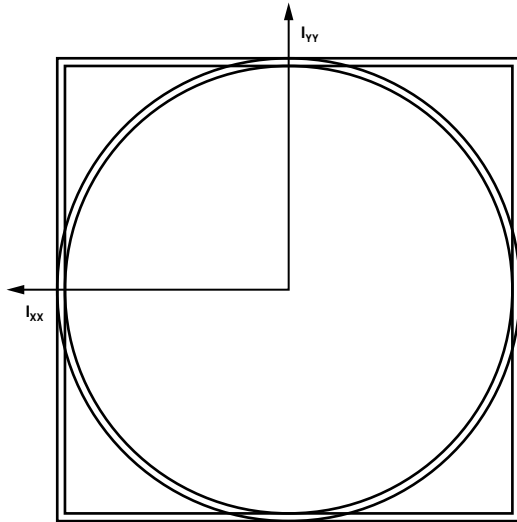


Figure 8. Area moment of inertia ( $I_{yy}$ ) and cross-sectional area.

The area moment of inertia,  $I_{yy}$ , of the rectangle is almost 50% greater than that of the cylinder, as shown in Table 3. The rectangle is better at withstanding deformation. However, the cross-sectional area,  $A$ , of the cylinder is three times larger than the rectangle. A larger  $A$  parameter means a larger fixed constraint both in simulation and reality—the cylinder is better designed for increased rigidity or higher stiffness.

Using the Table 3 values and Equation 5, the critical frequency is 60.74 kHz for the cylinder and 26.56 kHz for the rectangle. Equation 5 is a useful tool to show the relative performance of different geometries. Equations 4 and 5 predict four independent solutions below the critical frequency. Table 4 summarizes the FEM results and confirms the first four significant modes.

**Table 3. Area Moment of Inertia ( $I_{yy}$ ), Shear Modulus ( $G$ ), Density ( $\rho$ ), and Cross-Sectional Area ( $A$ ) for Cylinder and Rectangular Pieces**

Shape	$I_{yy}$ (m <sup>4</sup> )	$G$ (N/m <sup>2</sup> )	$\rho$ (kg/m <sup>3</sup> )	$A$ (m <sup>2</sup> )
Cylinder	6.24E-8	7.7E10	7850	1.03E-3
Rectangle	9.21E-8	7.7E10	7850	0.33E-3

**Table 4. First Four Significant Modes for Cylinder and Rectangle Shapes**

Mode	Cylinder (Hz)	Rectangle (Hz)
1	<b>11,890</b>	<b>5030.4</b>
2	<b>30,077</b>	10,559
3	40,506	<b>14,270</b>
4	50,777	<b>15,750</b>

**Bold** = mode participation factor > 0.1

Not bold = 0.01 < mode participation factor < 0.1

## What Is the Maximum Recommended Height for My Sensor?

Equations 4 and 5 are useful, but they do not provide analytical guidance on the trade-off between the vertical height of the enclosure and the first significant natural frequency possible. From Equation 2, we can intuitively see that the taller the sensor enclosure, the lower the first natural frequency.

### Limitations of Analytical Models

Equations 4 and 5 assume that the width of a beam cross section is at least 15% of the beam length.<sup>5</sup> Other approaches for long, thin beams, such as Bernoulli's equation,<sup>6</sup> assume that the width of beam cross section is less than 1% of the beam length.<sup>5</sup> For long, thin beams, Equation 6<sup>6</sup> can be used, which includes length ( $L$ ) or sensor height. Equation 6 does not consider shear forces, which are important for short, thick beams. For first significant natural frequencies, there is generally good agreement between equations 4, 5, and 6 for solid cylindrical shapes. For hollow shapes, Equation 6 underestimates the first significant natural frequency by 50%.

**Table 5. First Significant Mode for Hollow and Solid Cylinder Compared to Bernoulli's Equation**

30 mm Diameter Cylinder	Height/Length (mm)	Equation 6 (Hz)	Simulation (Hz)
Solid	60	5872	5267
Hollow, 2 mm wall	60	2930	5911

Equation 6<sup>6</sup> parameters include Young's modulus ( $E$ ) of stiffness, diameter ( $d$ ), length (or height), density of material used ( $\rho$ ), and  $K_n$  constants for given configurations.

$$f_n = \frac{K_n}{\pi} \sqrt{\frac{Ed^2}{16\rho L^4}} \quad (6)$$

As analytical models fail to provide guidance for height constraints for hollow enclosures, height studies typically rely on FEMs.

## Height Study

To provide guidance on performance degradation with increased enclosure height, the models shown in Figure 9 were simulated.

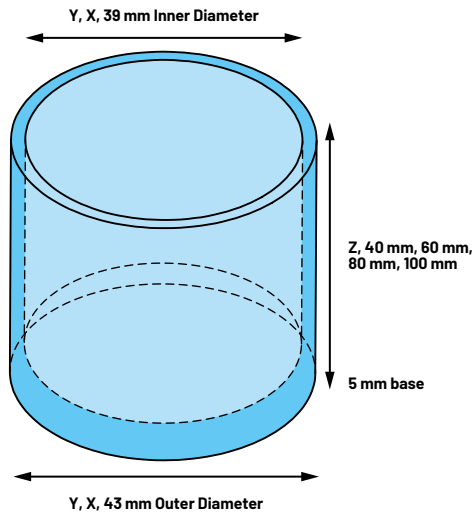


Figure 9. Height study for enclosure with 5 mm base.

The stainless steel extrusions include a 5 mm base, which can be used to provide a stud screw mount between the enclosure and monitored equipment (for example, a motor). Increasing the height of the cylinder from 40 mm to 100 mm results in a reduced first significant natural frequency of 12.5 kHz to 3.3 kHz for x and y axes, as shown in Figure 10. The z-axis also reduces from 31.2 kHz to 12.7 kHz. For high performance sensors it's clear that the enclosure height needs to be minimized.

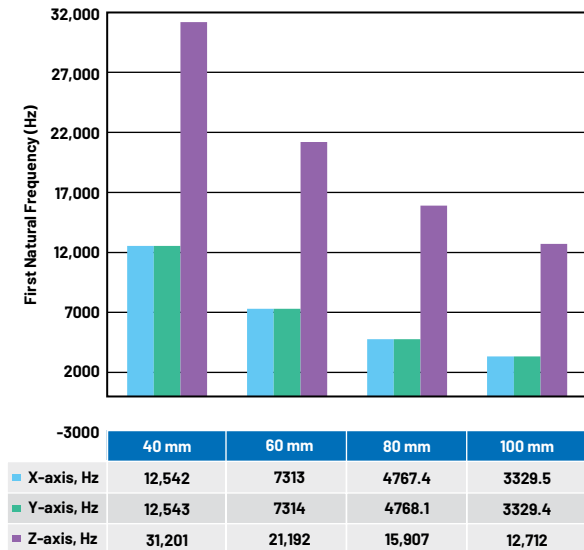


Figure 10. First significant natural frequency (Hz) for enclosure with 5 mm base and increased height.

## What Is the Effect of Reducing Enclosure Wall Thickness or Diameter?

### Reducing Enclosure Wall Thickness

Table 6 shows the geometric and material properties if the cylinder in Figure 6 is reduced from a 2 mm to a 1 mm wall thickness but keeps the 40 mm height and 43 mm outer diameter.

**Table 6. Area Moment of Inertia ( $I_{yy}$ ), Shear Modulus ( $G$ ), Density ( $\rho$ ), and Cross-Sectional Area ( $A$ ) for 1 mm and 2 mm Wall Thickness of a 40 mm Height Cylinder**

Shape	$I_{yy}$ ( $m^4$ )	$G$ ( $N/m^2$ )	$\rho$ ( $kg/m^3$ )	$A$ ( $m^2$ )
Cylinder, 2 mm wall	6.24E-8	7.7E10	7850	1.03E-3
Cylinder, 1 mm wall	3.12E-8	7.7E10	7850	5.28E-4

Using the Table 6 values and Equation 5, the critical frequency is 60.74 kHz for the 2 mm wall thickness cylinder and 61.48 kHz for the 1 mm wall thickness cylinder. With both  $I_{yy}$  and  $A$  parameters decreasing by about 50%, the numerator and denominator in Equation 5 are equally affected for the 1 mm wall thickness cylinder. From this calculation it is assumed that both cylinders will perform similarly in FEM modal analysis.

In Figure 11, the FEM results of first natural frequency with significant MPF (greater than 0.1 for the ratio of effective mass to total mass of the system) is plotted vs. cylinder wall thickness. The effect of reducing the cylinder wall thickness compared to natural frequency is very small.

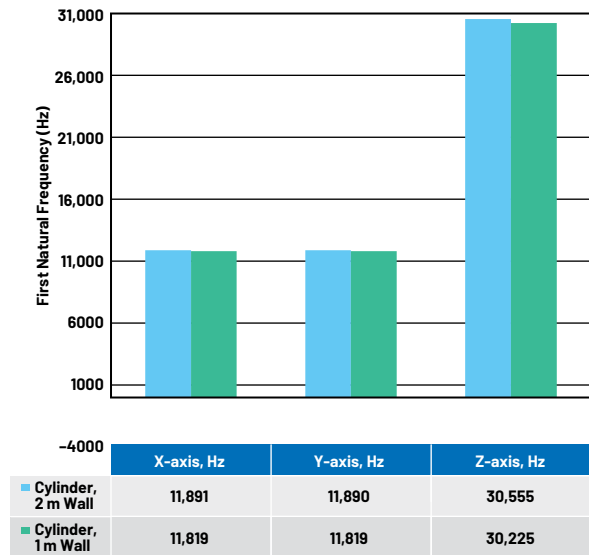


Figure 11. First significant natural frequency (Hz) for a cylinder with 1 mm or 2 mm wall thickness.

## Reducing Enclosure Diameter

The examples presented so far have all focused on cylindrical enclosures with a 43 mm outer diameter. Some designs may only require 30 mm or 26 mm outer diameters. Figure 12 illustrates the simulation model, and Figure 13 shows the effect of varying the outer diameter of the enclosure.

When reducing the cylinder diameter from 43 mm to 26 mm, the x and y axes' first natural frequencies reduce by about 1.5 kHz, while the z-axis first natural frequency increases by 1.9 kHz. In changing the cylinder diameter, both the area moment of inertia ( $I_{yy}$ ) and the cross-sectional area (A) decrease. The  $I_{yy}$  parameter will decrease more than the A parameter.

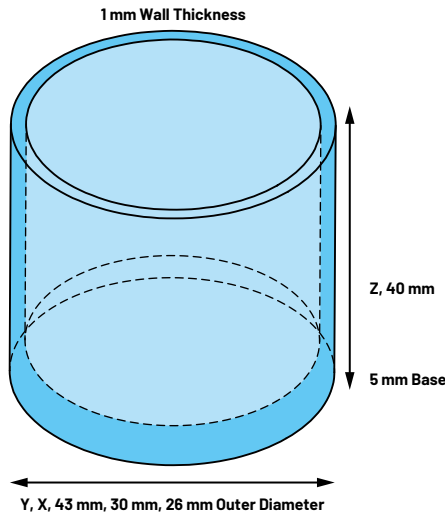


Figure 12. Enclosure diameter study.

In reducing the diameter from 43 mm to 30 mm, the  $I_{yy}$  will reduce by  $\frac{2}{3}$ , while the A will reduce by  $\frac{1}{3}$ . Again, referencing Equation 5, the net effect is a gradual decrease in first natural frequency. Intuitively, reducing the cylinder diameter will make the structure less rigid, so it makes sense that the natural frequency will reduce. However, using simulation it's clear that the reduction in first natural frequency is not dramatic, and changing diameters can still result in a first natural frequency in the tens of kHz.

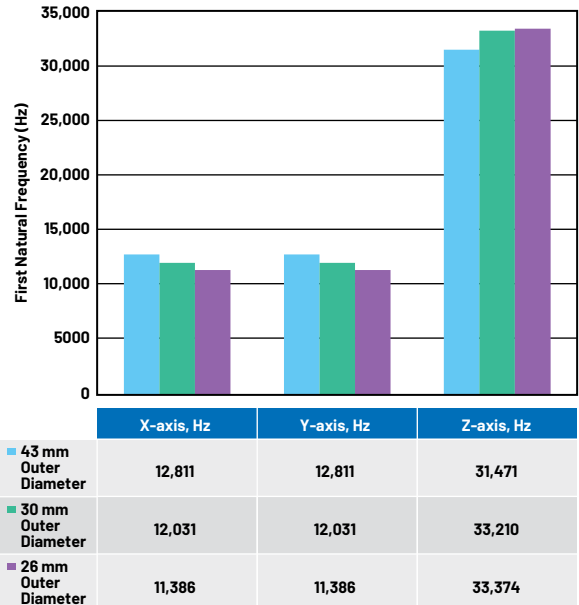


Figure 13. First significant natural frequency vs. cylinder outer diameter.

## Will Changing the Orientation of the Sensor Enclosure Increase Performance?

The previous sections of this article show that increasing the height of the enclosure will result in a reduced first natural frequency. It was also shown that using a cylindrical enclosure shape is recommended instead of using rectangular shapes. However, there are some cases where rectangular shapes are useful.

Consider a scenario where the enclosure needs to accommodate a sensor and circuit, with a defined 60 mm height, and 43 mm  $\times$  37 mm breadth and width. Using a rectangular shape and changing the orientation of fixed constraint (equipment attachment) can help to boost performance. The rectangular enclosure shown in Figure 14 has multiple attachment holes, so the enclosure can be mounted to equipment in various orientations. If the enclosure is mounted on the x, z face, then the effective height of the enclosure is 60 mm. However, if the enclosure is mounted on the y, z face, then the effective height is only 37 mm. This approach can be used for a rectangular enclosure, but not feasible using a cylinder's curved surface.

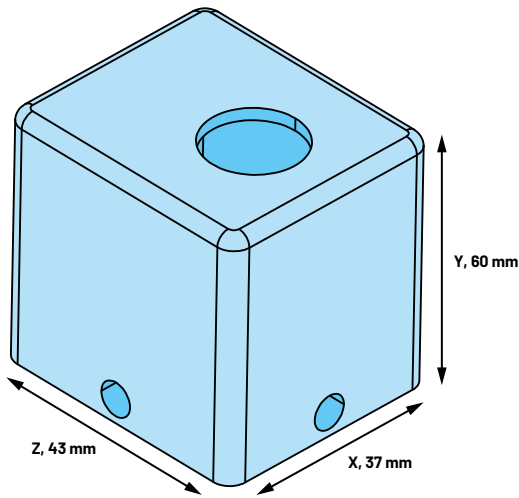


Figure 14. Rectangular enclosures can be constrained on the x and z axes, or on the y and z axes to reduce height.

Figure 15 shows that by changing the enclosure orientation, the x-axis first resonant frequency can be boosted, and the y-axis is better when compared to a cylinder. The z-axis first resonant frequency is higher for the y, z fixed orientation compared to the x, z fixed orientation, with almost double the frequency mode. However, the cylinder performs the best by far for z-axis natural frequency. A rectangular shape is a good approach to have similar performance across three axes in comparison to a cylindrical shape.

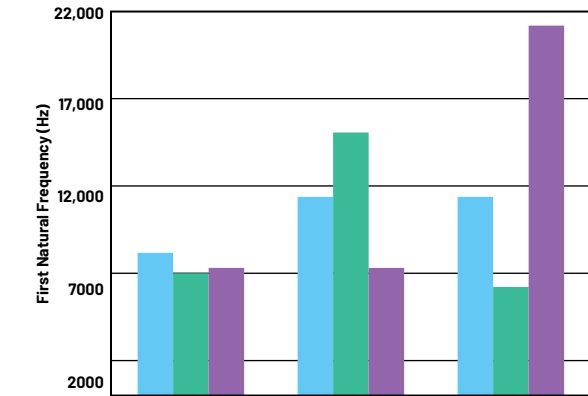


Figure 15. First significant natural frequency vs. cylinder or rectangular shape orientation.

## Single-Axis 11 kHz MEMS Sensor with 21 kHz Resonance

Based on the simulation and analytical results presented in this article, a cylindrical enclosure will perform best for housing a single-axis ADXL1002 MEMS sensor with 21 kHz resonance. The MEMS sensor axis of sensitivity should be orientated to take advantage of the cylindrical enclosure's first natural frequency performance in the z-axis.

### Enclosure Prototype and Assembly Concept

The simulation models presented so far have excluded connector choices and their influence on the natural frequencies of the enclosure design. Figure 16 shows an M12 4-wire connector, part number T4171010004-001 from TE. This connector is IP67 rated for water and dust resistance and includes a .STEP file from TE that can easily be integrated into the enclosure design file. This connector can be used with an M12-to-M12 cable, such as the TAA545B1411-002 from TE.

A good mechanical mounting is critical to ensure the best transfer of vibration and avoid resonances that may affect performance. A good mounting is typically achieved using a stud threaded to both sensor enclosure and monitored equipment. The stainless steel model shown in Figure 16 includes a solid 7 mm base with an industry-standard 1/4"-28 threaded hole for mounting the stud attachment to the monitored equipment.

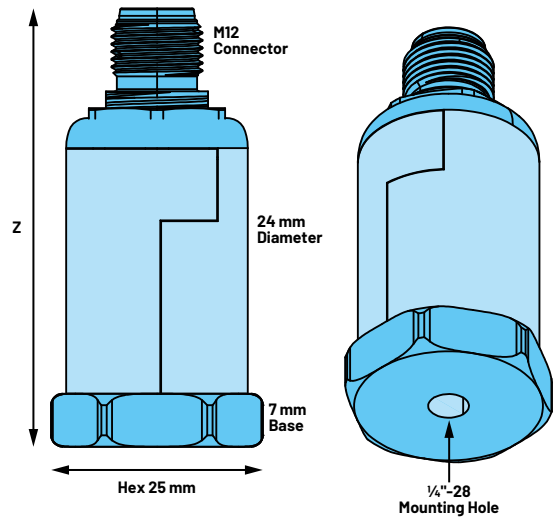


Figure 16. Enclosure prototype.

The enclosure measures 24 mm in diameter and includes a hexagonal 25 mm base, which can be used to torque the sensor into the monitored equipment. The total height of the enclosure with M12 connector can be varied between 48 mm and 57 mm, depending on manufacturing tolerances and assembly of internal wiring or soldering options from the connector to the MEMS PCB. For example, at least 5 mm of height is needed if using a straight wire connection between the M12 cap and the MEMS PCB.

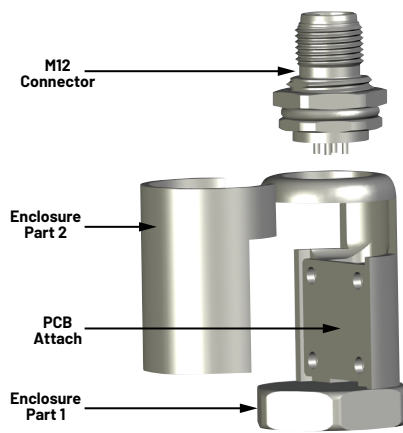


Figure 17. One possible assembly concept for MEMS sensor PCB, M12 connector, and enclosure.

Figure 17 shows an exploded view of one possible assembly option for the enclosure, M12 connector, and MEMS PCB. The MEMS PCB can be assembled to the enclosure wall using M3 screws, then attached to the M12 connector, and then finally the two enclosure pieces can be laser welded together. The PCB is vertically mounted as shown, with the ADXL1002 MEMS axis of sensitivity aligned vertically with the z-axis of the enclosure. A vertical mount is also important from a system measurement perspective, as this orientation is usually required for measuring bearing faults (for example, radial vibration measurements) on motors.

### Modal Simulation

Before modal simulation, one solid body should be created using the components shown in Figure 17. This will provide a simulation model that closely matches an assembled and welded sensor. A fine mesh should be selected for accurate FEM numerical simulation, especially for the connector geometry. The Fine Span Angle Center ANSYS Mesh option should be selected for best performance. Figure 18 shows the FEM mesh and relative deformation of the enclosure after simulation.

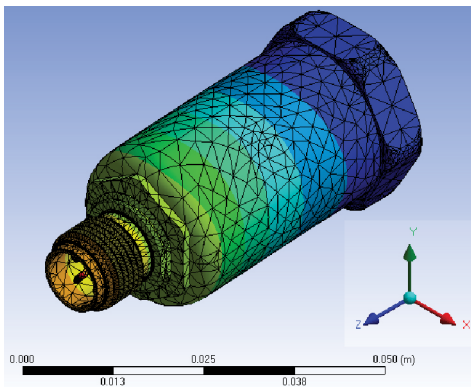


Figure 18. FEM mesh detail and relative deformation of the enclosure.

The gradual gradient from blue to orange and red in Figure 18 illustrates the larger relative structural deformation at the top of the enclosure and the connector.

Figures 19 and 20 show the FEM results for first natural frequency with significant MPF (greater than 0.1 for the ratio of effective mass to total mass of the system) vs. total sensor height for the z-axis. The z-axis performance is critical, with

19.38 kHz for first significant natural frequency when the enclosure height is at 52 mm. For 48 mm total height the performance improves to 22.44 kHz. A 50 mm height enclosure will give around 21 kHz performance.

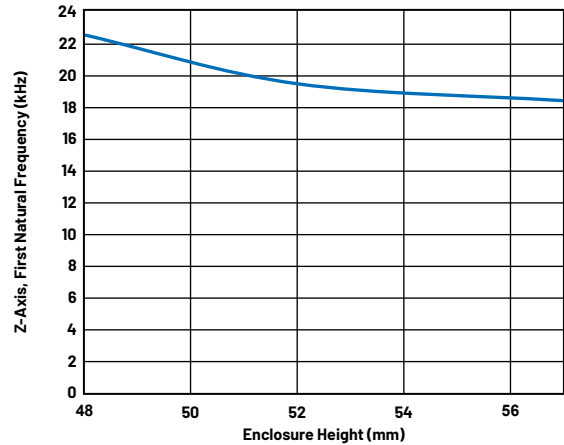


Figure 19. First significant natural frequency (z-axis) vs. enclosure height.

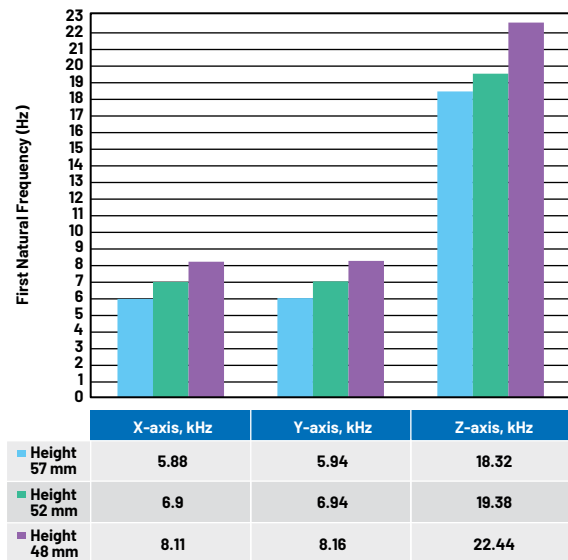


Figure 20. First significant natural frequency vs. enclosure height (x, y, and z axes).

### Triaxial 10 kHz MEMS Sensor with 21 kHz Resonance

Controlling the natural frequency of an enclosure design across three axes is a more difficult task compared to a single-axis sensor, particularly when 21 kHz performance is required.

#### ADcmXL3021

Fortunately, Analog Devices has developed the **ADcmXL3021**  $\pm 50$  g, 10 kHz, triaxial, digital output MEMS vibration sensing module, as shown in Figure 21. The ADcmXL3021 is available in a 23.7 mm  $\times$  27.0 mm  $\times$  12.4 mm aluminum package with four mounting flanges to support installation with standard M2.5 machine screws. The ADcmXL3021 package aluminum material and geometry support resonant frequencies of greater than 21 kHz across x, y, and z axes.

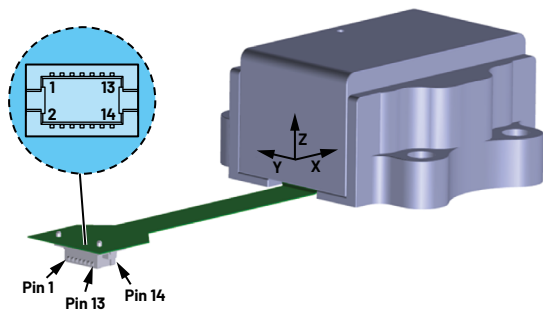


Figure 21. ADcmXL3021 triaxial digital output MEMS in aluminum package with flex connector.

### Adding the ADcmXL3021 to an IP67 Rated Enclosure

An IP67 rated (water and dust proof) enclosure and connector are required for placing the ADcmXL3021 in industrial environments. In addition, the SPI output from the ADcmXL3021 is not suitable for use with long cables. The SPI output needs to be converted for long cable driving, using Industrial Ethernet or RS-485 transceiver circuits.

Based on the studies in this article, it's not possible to place the ADcmXL3021, the RS-485 or Ethernet PCB, and a connector in the same enclosure and achieve 21 kHz resonant frequencies across all three (x, y, and z) axes. The combination of components will result in a minimum enclosure size like that shown previously in Figure 2 (40 mm × 43 mm × 37 mm). Figure 2 provided a first significant natural frequency of around 10 kHz to 11 kHz across three axes. In addition, Figure 2 was not simulated using a connector, which will increase the effective height and reduce the natural frequencies further.

If a simple rectangular aluminum shape is simulated using FEM, with 23.7 mm × 27 mm × 12.4 mm dimensions (like the ADcmXL3021) and 2 mm wall thickness, the first significant natural frequency exceeds 21 kHz across all axes.

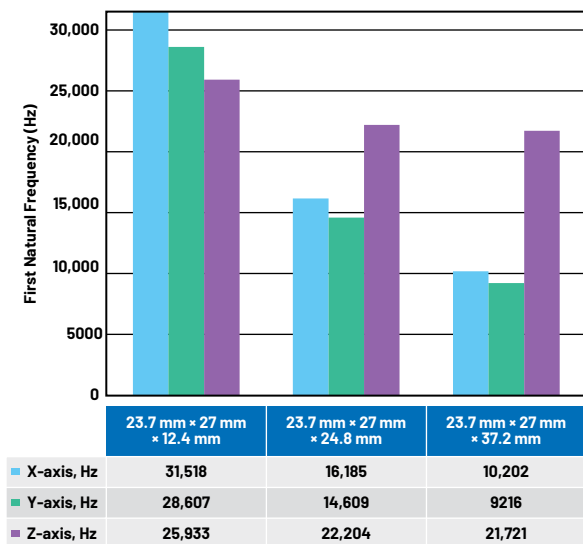


Figure 22. Increasing the height of a shape like the ADcmXL3021.

When the 12.4 mm height is doubled and tripled to provide space for additional circuitry, the natural frequency reduces significantly, as shown in Figure 22. Even with just a 12.4 mm allowance for additional circuitry, the first significant natural frequency falls below 15 kHz.

### A Distributed System

Instead of trying to fit all components into one rectangular enclosure, a distributed system like Figure 23 is suggested. Using this concept, the ADcmXL3021 is housed in an IP67 rated enclosure, with SPI data routed over a short distance (less than 10 cm) to a separate IP67 enclosure, which houses the cable interface PCBs with Ethernet or RS-485 transceiver, as well as associated power supply IC and other circuitry.

Using this approach, the geometry is significantly reduced, and the problem of matching the enclosure's natural frequency to that of the ADcmXL3021 is significantly easier.

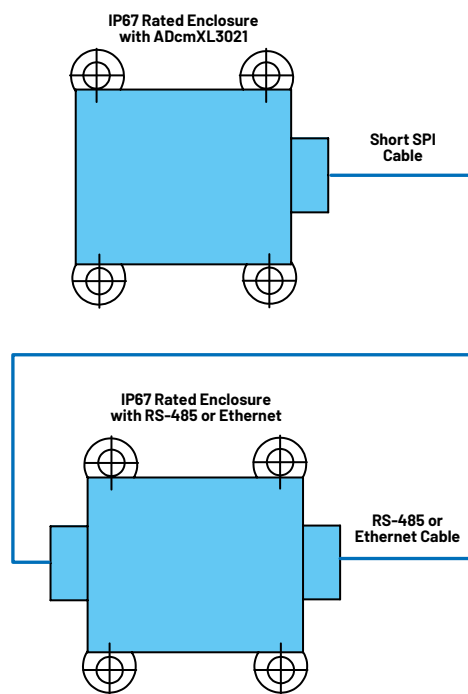


Figure 23. The ADcmXL3021 and interface circuits are housed in separate enclosures.

### Design and Modal Analysis

As shown previously, a rectangular shape is a good approach to achieve similar natural frequency performance across three axes in comparison to a cylindrical shape. In Figure 23, the ADcmXL3021 is placed in a small, hollow, rectangular enclosure with a tiny PCB to interface between the ADcmXL3021 flex cable and industrial connector. A small profile M8 connector, such as TE 7-1437719-5, can be used with the model. The rectangular enclosure includes four M2.5 mounting holes, to provide a fixed mounting to equipment. The total enclosure size is

40.8 mm × 33.1 mm × 18.5 mm. Critically, the z-axis height is 18.5 mm, which helps to achieve higher frequency modes.

The Figure 24 y, x face and four M2.5 holes are constrained for modal simulation. The z direction is the weakest link in the design, even at sub-20 mm heights. Figure 25 shows one of the FEM modal simulation dominant modes, which illustrates the larger relative structural deformation at the top of the enclosure.

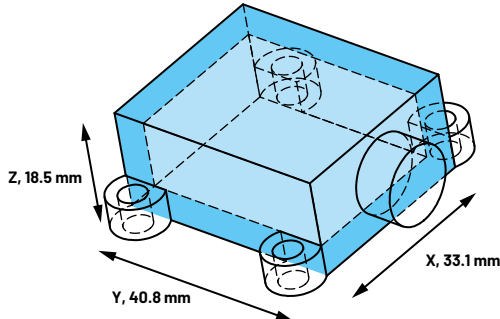


Figure 24. Hollow enclosure used to house the ADcmXL3021.

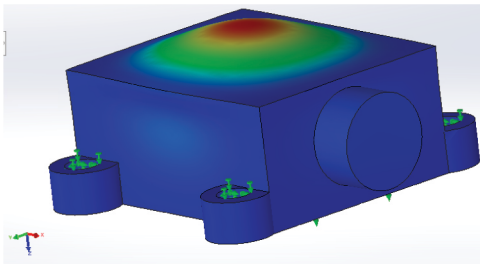


Figure 25. Dominant mode from simulation for the hollow enclosure used to house the ADcmXL3021.

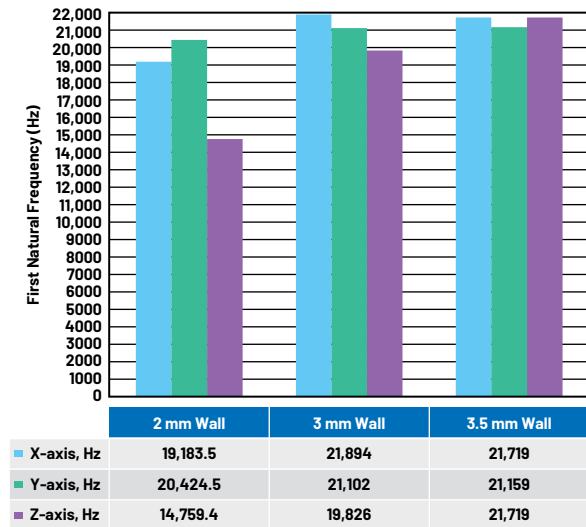


Figure 26. First significant natural frequency vs. wall thickness for the z-axis.

The z direction stiffness can be increased by increasing the wall thickness. For example, if 2 mm wall thickness is used, the z direction's first significant natural frequency is at 14.76 kHz. When a 3 mm wall thickness is used, this increases to 19.83 kHz. As shown in Figure 26, using a 3.5 mm wall thickness provides greater than 21 kHz natural frequency in the z direction.

## Adding Epoxy in the Enclosure

Epoxy resin can be added to vibration sensor enclosures to hold hardware PCBs in a fixed position, and to prevent movement of connectors and internal wiring.

To study the effects of epoxy resin on the natural frequency of an enclosure, a simple FEM model was created with a 40 mm × 40 mm hollow, stainless steel cube of fixed 2 mm wall thickness. The cube was filled with 36 mm × 36 mm epoxy resin. The height of the enclosure was increased from 40 mm to 80 mm to 100 mm, and alternate simulations were performed with and without the epoxy fill. The FEM simulations were performed with the x, y surface as the fixed constraint.

Table 7 presents the simulation results, with some interesting findings:

- ▶ For smaller sensor heights, and where the height is equal to the length/width, the epoxy resin boosts the first significant natural frequency in the cantilevered axis (z) by up to 75%.
- ▶ Where the sensor height of 80 mm is 2× the length/width, the first significant natural frequency in the cantilevered axis (z) increases by 16% when using an epoxy resin fill. However, the x and y radial axes reduce by 10%.
- ▶ As the height increases to 3× of the length/width, the epoxy resin reduces the first significant natural frequency.

**Table 7. Height (mm), Epoxy Fill (Yes/No), and First Significant Natural Frequency for a 2 mm Wall Thickness of a 40 mm (Length) × 40 mm (Width) Stainless Steel Cube**

Height (mm)	Epoxy Fill?	X Freq. (Hz)	Y Freq. (Hz)	Z Freq. (Hz)
40	No	8547	8450	9291
40	Yes	8586	8585	16,259
80	No	3943	3943	9716
80	Yes	3567	3530	11,272
120	No	2208	2208	9293
120	Yes	1906	1906	8045

As height increases, the mass increases and the stiffness decreases. At a certain point, the mass increase has a greater influence than the added epoxy stiffness. For the given simulation example, this inflection point is at greater than 80 mm. However, most sensors are usually less than 80 mm in height. So, it can be concluded that, for most cases, adding epoxy resin will aid the natural frequency performance for a vibration sensor enclosure solution.

## External Cable Simulation

After mounting a vibration sensor on a machine surface, the cable should be anchored to reduce stress at cable terminations and to prevent false signals due to cable vibration. When securing the cable, leave enough slack to allow free movement of the accelerometer.<sup>7</sup>

This section simulates the effect of a vibrating cable on system response and provides guidance as to where the cable should be clamped (at what cable length).

A simulation model was created, with the material properties as shown in Figure 27. TE provides connector and cable models, such as the TAA545B1411-002, which can be used as a baseline. The cable connector is made from Nylon (Nylon 6/6), with copper cable wire and PVC insulation. The attached sensor is designed using stainless steel and filled with epoxy resin. The simulation model is supported with a fixed constraint on the sensor attach, and the 0.15 m cable is free to vibrate along its length. The 0.15 m cable length can be increased to 1 m for simulation.

Table 8 provides the simulation results, with some key findings:

- ▶ If the cable is clamped at less than 0.15 m length, then the cable effect on the vibration sensor frequency response is minimal. Both with and without a 0.15 m cable the frequency response of the sensor enclosure is above 11 kHz.
- ▶ If 1 m of cable is attached to the sensor, and allowed to move freely and vibrate along its entire length, then the added cable mass will dominate the system frequency response. The cable frequency response of 500 Hz will become the dominant mode.

In reality, it is unlikely that an entire 1 m cable will vibrate, as the vibration will be dampened with increased cable length. However, this simulation example shows that anchoring at around 0.15 m is a good idea for accurate system response.

**Table 8. Cable Length (m) and First Significant Natural Frequency (Hz), With and Without a Connected Vibration Sensor Enclosure**

Cable Length (m)	Sensor Used in Simulation?	Z Frequency (Hz)
1	Yes	464
1	No	508
0.15	Yes	11,272
0.15	No	11,568

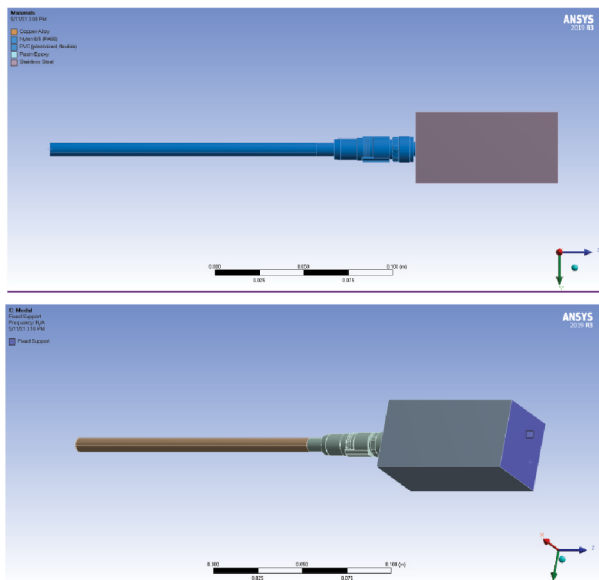


Figure 27. Cable and sensor model with material properties and 0.15 m cable length.

## Vibration Sensor Mounting

Figure 28 shows the effect on mounting resonance and typical usable frequency range for the stud, adhesive, adhesive mounting pad, and flat magnet techniques shown in Figure 29. Stud and adhesive mounting places the sensor as close as possible to the machine, with best coupling of vibration signal from machine to MEMS sensor. Using a fixture with an adhesive mounting pad places additional metal material between the machine and sensor. This additional material dampens the frequency response of the sensor solution. The flat magnet mount also dampens the frequency response and does not provide as good a fixed attachment to the equipment as the other methods.

Figure 28 provides typical guidelines only, and each sensor should be characterized via lab measurement or simulation.

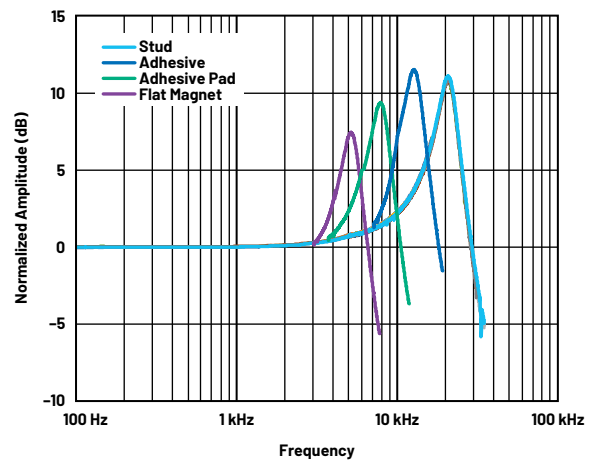


Figure 28. Effect of mounting technique on sensor resonance.

Simulation of stud mounting with ANSYS modal analysis is performed using the default bonded contact constraint. This is where the bottom of the vibration sensor—and, in particular, the ¼”-28-inch mounting hole—is designated as a fixed constraint using ANSYS. The constraint type is default bonded or a bolted connection.

Simulation of adhesive contact is an advanced topic and requires ANSYS cohesive zone modeling (CZM) and an understanding of contact mechanics. For accuracy, the ANSYS CZM requires parameters input based on lab test data. For example, the article “Direct Measurement of the Cohesive Law of Adhesives Using a Rigid Double Cantilever Beam Technique”<sup>6</sup> can be used for inputs to ANSYS. If you don’t find experimental data published for your chosen adhesive, then you will need to do some lab measurements. In addition, the correct contact formulation needs to be set up in ANSYS, with guidance provided in short courses such as *Fundamental Topics in Contact*.<sup>9</sup> Finally, the CZM and modal techniques then need to be combined within the ANSYS workbench.

ANSYS Maxwell<sup>10</sup> can be used to simulate magnetic fields. However, as magnetic forces are noncontact forces (they push or pull objects without “solid” contact), generating an appropriate contact constraint for numerical modal analysis is not possible. Modal analysis can be performed with bonded, frictionless, frictional, and no separation contacts. CZM contact may also be possible, as mentioned previously.

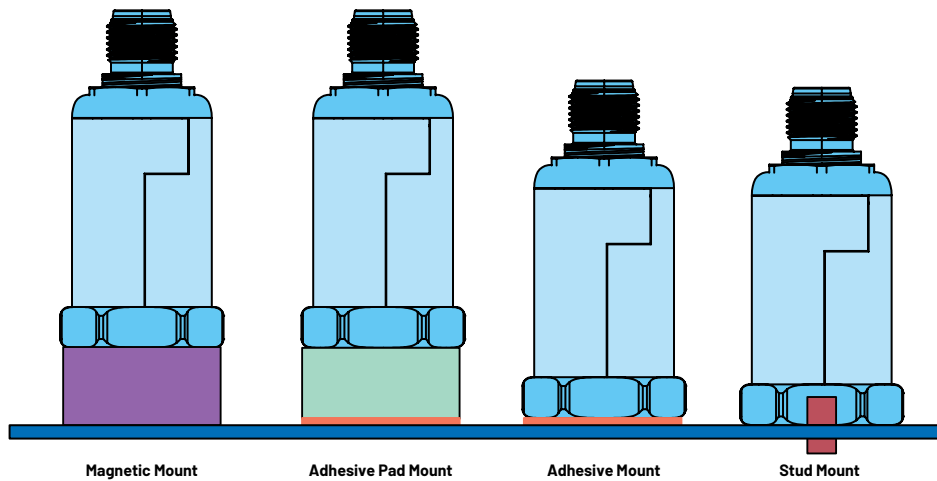


Figure 29. Mounting techniques for vibration sensors.

## Conclusion

A good mechanical enclosure design for a MEMS accelerometer will ensure that high quality vibration data for CbM is extracted from the monitored asset.

Designing a good mechanical enclosure for MEMS accelerometers requires an understanding of modal analysis. Modal analysis provides the natural frequencies in the axis of interest for a vibration sensor enclosure. In addition, the mode participation factor (MPF) will enable the designer to decide if a frequency can be ignored in a design.

Both material characteristics and geometry need to be considered when designing a vibration sensor enclosure to meet natural frequency targets. Enclosure height needs to be minimized to achieve higher natural frequencies. Reducing wall thickness or enclosure diameter both have secondary effects on the enclosure natural frequencies.

Cylindrical shapes with higher cross-sectional areas are better designed for higher rigidity and natural frequencies across all axes, compared to rectangular shapes. Rectangular shapes offer more options in sensor orientation and equipment attachment, compared to cylindrical shapes. Rectangular shapes are useful in maintaining similar natural frequency performance across three axes.

For most cases, adding epoxy resin will aid the natural frequency performance for a vibration sensor enclosure solution. Using stud or adhesive mounting provides the best usable frequency range for a vibration sensor, while using magnetic or adhesive pads reduces sensor performance.

## References

- <sup>1</sup> ANSYS Innovation Courses: Modal Analysis. ANSYS, 2021.
- <sup>2</sup> Stephen Timoshenko. *Vibration Problems in Engineering*, 4<sup>th</sup> edition. John Wiley and Sons Inc., New York, 1974.
- <sup>3</sup> Leszek Majkut. "Free and Forced Vibrations of Timoshenko Beams Described by Single Difference Equation." *Journal of Theoretical and Applied Mechanics*, Vol. 47, No. 1, January 2009.

- <sup>4</sup> Mohammad Hossein Abolbashari, Somayeh Soheili, and Anoshirvan Farshidianfar. "Flexural Vibration of Propeller Shafts Using Distributed Lumped Modeling Technique." The 16<sup>th</sup> International Congress on Sound and Vibration, Krakow, 2009.
- <sup>5</sup> Saida Hamioud and Salah Khalfallah. "Spectral Element Analysis of Free - Vibration of Timoshenko Beam." *International Journal of Engineering*, 2018.
- <sup>6</sup> Olivier A. Bauchau and James I. Craig. *Structural Analysis: With Applications to Aerospace Structures*, Springer, 2009.
- <sup>7</sup> TN17: Installation of Vibration Sensors, Wilcoxon Sensing Technologies, 2018.
- <sup>8</sup> A. Khayer Dastjerdi, E. Tan, and F. Barthelat. "Direct Measurement of the Cohesive Law of Adhesives Using a Rigid Double Cantilever Beam Technique." Society for Experimental Mechanics, May 2013.
- <sup>9</sup> ANSYS Innovation Courses: Fundamental Topics in Contact. ANSYS, 2021.
- <sup>10</sup> Ansys Maxwell: Low Frequency EM Field Simulation. ANSYS, 2021.

## About the Author

Richard Anslow is a system applications engineer with the Connected Motion and Robotics Team within the Automation and Energy Business Unit at Analog Devices. His areas of expertise are condition-based monitoring and industrial communication design. He received his B.Eng. and M.Eng. degrees from the University of Limerick, Limerick, Ireland. He can be reached at [richard.anslow@analog.com](mailto:richard.anslow@analog.com).

Engage with the ADI technology experts in our online support community. Ask your tough design questions, browse FAQs, or join a conversation.

  
SUPPORT COMMUNITY

Visit [ez.analog.com](https://ez.analog.com)



AHEAD OF WHAT'S POSSIBLE™

For regional headquarters, sales, and distributors or to contact customer service and technical support, visit [analog.com/contact](https://analog.com/contact).

Ask our ADI technology experts tough questions, browse FAQs, or join a conversation at the EngineerZone Online Support Community. Visit [ez.analog.com](https://ez.analog.com).

©2022 Analog Devices, Inc. All rights reserved. Trademarks and registered trademarks are the property of their respective owners.

TA23321-2/22

VISIT [ANALOG.COM](https://analog.com)